Tumor suppressor miR-375 regulates MYC expression via repression of CIP2A coding sequence through multiple miRNA–mRNA interactions

Hyun Min Jung[a], Rushi S. Patel[a], Brittany L. Phillips[a], Hai Wang[b], Donald M. Cohen[c], William C. Reinhold[d], Lung-Ji Chang[e], Li-Jun Yang[b], and Edward K. L. Chan[a]

[a]Department of Oral Biology, [b]Department of Pathology, [c]Department of Oral and Maxillofacial Diagnostic Sciences, and [e]Department of Molecular Genetics and Microbiology, University of Florida, Gainesville, FL 32610; [d]Laboratory of Molecular Pharmacology, Center for Cancer Research, National Cancer Institute, National Institutes of Health, Bethesda, MD 20814

ABSTRACT **MicroRNAs (miRNAs) are small, noncoding RNAs involved in posttranscriptional regulation of protein-coding genes in various biological processes. In our preliminary miRNA microarray analysis, miR-375 was identified as the most underexpressed in human oral tumor versus controls. The purpose of the present study is to examine the function of miR-375 as a candidate tumor suppressor miRNA in oral cancer. Cancerous inhibitor of PP2A (CIP2A), a guardian of oncoprotein MYC, is identified as a candidate miR-375 target based on bioinformatics. Luciferase assay accompanied by target sequence mutagenesis elucidates five functional miR-375–binding sites clustered in the CIP2A coding sequence close to the C-terminal domain. Overexpression of CIP2A is clearly demonstrated in oral cancers, and inverse correlation between miR-375 and CIP2A is observed in the tumors, as well as in NCI-60 cell lines, indicating the potential generalized involvement of the miR-375–CIP2A relationship in many other cancers. Transient transfection of miR-375 in oral cancer cells reduces the expression of CIP2A, resulting in decrease of MYC protein levels and leading to reduced proliferation, colony formation, migration, and invasion. Therefore this study shows that underexpression of tumor suppressor miR-375 could lead to uncontrolled CIP2A expression and extended stability of MYC, which contributes to promoting cancerous phenotypes.**

Monitoring Editor
Kunxin Luo
University of California, Berkeley

Received: Dec 20, 2012
Revised: Mar 20, 2013
Accepted: Mar 26, 2013

INTRODUCTION

MicroRNAs (miRNAs) are endogenous small, noncoding RNAs that play roles as posttranscriptional regulators of gene expression involved in diverse physiological and pathological processes (Ambros, 2004; Bartel, 2009). About 60% of all mammalian mRNAs are estimated targets of miRNAs, indicating significant roles of miRNAs in the regulation of diverse cellular processes such as proliferation, differentiation, development, and cell death (Friedman *et al.*, 2009). In cancer research, miRNAs play critical role in either promoting or suppressing carcinogenesis (Esquela-Kerscher and Slack, 2006). The development of profiling methods for miRNA expression analyses revealed a number of deregulated miRNAs in various types of cancers (Lu *et al.*, 2005; Volinia *et al.*, 2006). Discovery of miRNAs and exploration of their functions in cancer biology are rapidly developing fields (Garzon *et al.*, 2010; Sun *et al.*, 2010). Many miRNAs exhibit altered expression levels in cancer, and cancer biologists are only starting to understand the functional consequences of the loss or gain of particular miRNAs to the cancerous phenotype (Voorhoeve and Agami, 2007).

This article was published online ahead of print in MBoC in Press (http://www.molbiolcell.org/cgi/doi/10.1091/mbc.E12-12-0891) on April 3, 2013.

Address correspondence to: Edward K. L. Chan (echan@ufl.edu).

Abbreviations used: CDS, coding sequence; CIP2A, cancerous inhibitor of PP2A; FL, firefly luciferase; miRNA, microRNA; NS control, nonspecific control; SCC, squamous cell carcinoma; UTR, untranslated region.

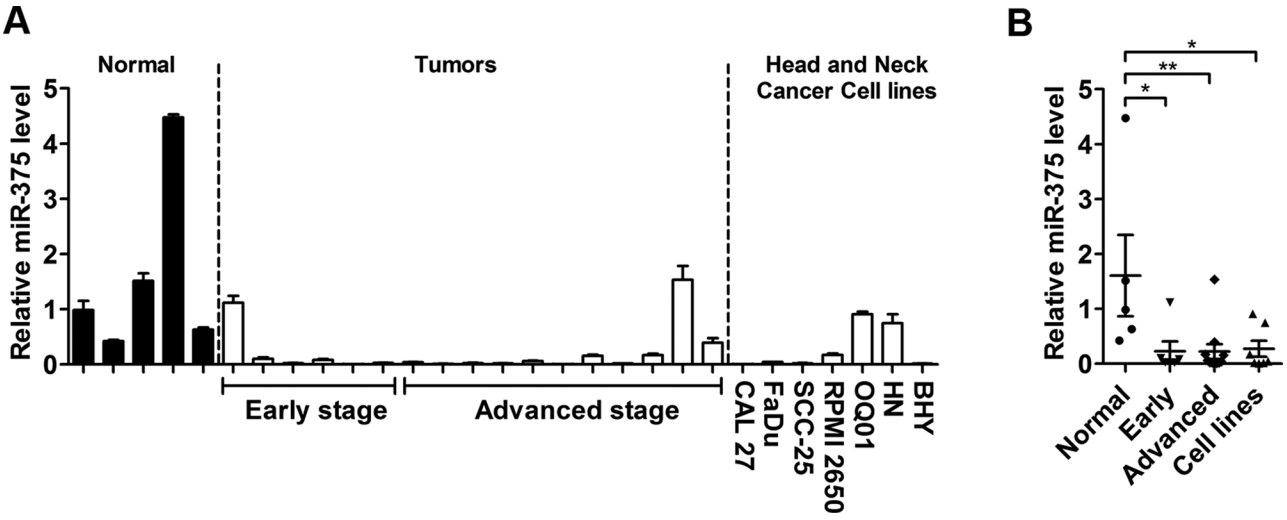

FIGURE 1: miR-375 is underexpressed in oral cancer. (A) Expression levels of miR-375 in human oral tissues (five normal controls and 17 tumors) and in seven head and neck cancer cell lines measured by quantitative real-time PCR (qRT-PCR). Tumors were subgrouped by early-stage ($n = 6$) and advanced-stage ($n = 11$) tumors. (B) The overall level of miR-375 was further analyzed to determine statistical differences. All qRT-PCR results are expressed as mean ± SEM from at least three independent experiments. *$p < 0.05$; **$p < 0.01$.

Oral cancer is a significant global disease, with an estimated ~300,000 new cases and 130,000 deaths annually worldwide (Jemal *et al.*, 2011). Although the incidence of oral cancer comprises around 3% of all new cases of cancer worldwide, this disease is considered a critical public health threat due to the relatively low survival rate (~50%) among the major cancers (Messadi *et al.*, 2009). Oral carcinogenesis occurs by a multistep process in which accumulation of genetic or epigenetic modifications, such as loss of heterozygosity and aberrant gene expression, contributes to cancer development (Lippman *et al.*, 2005). At early stages, oral cancers can be treated by surgery or radiation therapy alone, with 5-yr survival rate of ~80%, whereas this drops to ~30% for advanced-stage oral cancers due to the failure of response even to combined therapies (Funk *et al.*, 2002; Howlader *et al.*, 2012). Despite the identification of many molecular-level basics involved in these pathogenesis processes, the 5-yr survival rate for oral cancer has not improved for several decades (Jemal *et al.*, 2011). The limited information available at the molecular levels of oral carcinogenesis and the biological heterogeneity of these cancers hamper the development of new therapeutic strategies. Therefore there is an urgent need for understanding the molecular pathogenesis of the disease and developing targeted therapeutic strategies based on identified mechanisms for oral carcinogenesis.

Our previous studies identified a novel 90-kDa autoantigen (p90) overexpressed in hepatocellular carcinomas, gastric cancer, and prostate cancer (Soo Hoo *et al.*, 2002; Shi *et al.*, 2005). A collaborative study in 2007 illustrated a crucial function of this protein to inhibit protein phosphatase 2A (PP2A) activity toward MYC serine 62 by directly interacting with MYC and as a result preventing proteolytic degradation of MYC (Junttila *et al.*, 2007). Based on its newly identified function, p90 was named cancerous inhibitor of PP2A (CIP2A). Since the first recognition of p90 as a tumor biomarker in 2002, elevated expression of p90/CIP2A (hereafter CIP2A) has been reported in various types of cancer, indicating an important contribution of this protein during carcinogenesis (Soo Hoo *et al.*, 2002; Shi *et al.*, 2005; Junttila *et al.*, 2007; Li *et al.*, 2008; Come *et al.*, 2009; Katz *et al.*, 2010; Dong *et al.*, 2011; Ren *et al.*, 2011). MYC is a transcription factor implicated in the activation and/or repression of hundreds of genes involved in proliferation, growth, differentiation, and cell death (Fernandez *et al.*, 2003). Due to its critical role, deregulation of MYC is estimated in up to 70% of human cancers (Dang, 2012). Deregulated MYC expression results in constitutive expression of MYC protein, which has been linked to genomic instability (Prochownik, 2008) and further contributes to tumorigenesis (Dang, 2012). Despite the natural short half-life of MYC protein, its life can be extended by CIP2A in human malignancies (Junttila *et al.*, 2007; Junttila and Westermarck, 2008). As a result, elevated expression of MYC accompanied by CIP2A overexpression promotes cell transformation and tumor progression.

In the present study, we show that miR-375 is a tumor suppressor miRNA inhibiting cancerous properties such as proliferation, migration, and invasion in oral cancer. In addition, we identify CIP2A as a novel miR-375 target, which is regulated via posttranscriptional control through multiple binding sites on the coding region of CIP2A and accordingly stabilizes the oncogenic protein MYC.

RESULTS

miR-375 is underexpressed in oral cancer

About 90% of all oral cancers consist of squamous cell carcinomas (SCCs; van der Waal *et al.*, 2011), and tongue cancer is the major type of oral cancer (Shiboski *et al.*, 2000). Therefore SCCs from tongues were mainly selected in this study to represent the major subtype of oral cancer. In our previous miRNA microarray analyses, deregulated miRNAs in oral cancer were identified (Jung *et al.*, 2012). Among those miRNAs, miR-375 was the most underexpressed miRNA in the oral tumors. In particular, a majority of oral tumors (88%, 15 of 17) and head and neck cancer cell lines (71%, five of seven) expressed lower miR-375 levels than any normal controls (Figure 1A). Overall, miR-375 was significantly underexpressed in the oral tumors, regardless of the tumor stage, as well as in seven head and neck cancer cell lines compared with normal controls (Figure 1B). Our data, consistent with previous reports of underexpression of miR-375 in various cancers, suggest that miR-375 is a potential tumor suppressor in oral cancer and that the absence of miR-375 might play a role during the development of oral cancer.

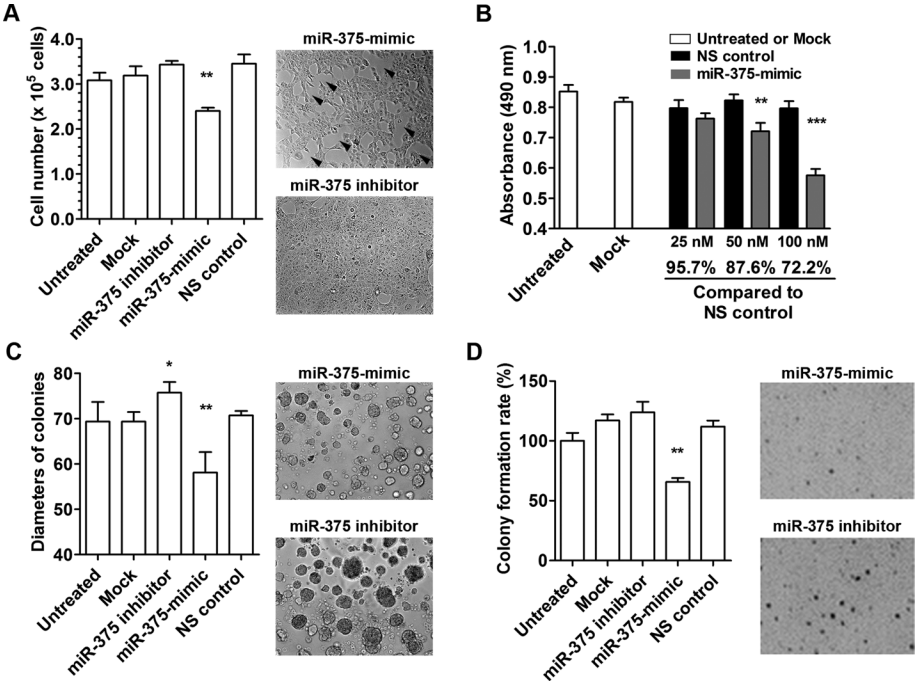

FIGURE 2: miR-375 suppresses oral cancer cell proliferation and colony formation. (A) The cells were counted 72 h posttransfection by trypan blue exclusion staining assay. Representative images are CAL 27 cells transfected with miR-375-mimic or miR-375 inhibitor. Arrowheads indicate sparse areas only observed in the plate with miR-375-mimic–transfected cells. (B) Cell proliferation rate was measured 72 h posttransfection of miR-375-mimic in different doses (25, 50, 100 nM) using MTS assay. The proliferation rates of miR-375-mimic–transfected cells were compared with that of NS control–transfected cells. (C) Transfected cells were seeded on 1:1 diluted Matrigel, and images of live-cell colonies were taken after growth in Matrigel for 4 d. Diameters of 150 colonies from three independent experiments were measured using AxioVision, release 4.7, software. (D) Soft agar colony formation assay–determined anchorage-independent tumor growth was reduced by miR-375-mimic transfection. *$p < 0.05$; **$p < 0.01$; ***$p < 0.001$.

miR-375 suppresses oral cancer cell proliferation

To investigate the effects of miR-375, we used CAL 27 cells derived from a tongue cancer for in vitro studies. After 72 h of transfection, trypan blue exclusion assay was performed to measure proliferation rate. Significantly reduced proliferation was observed in the miR-375-mimic–transfected cells compared with cells untreated, treated with mock condition, transfected with miR-375 inhibitor, or non-specific (NS) control (Figure 2A). A 3-(4,5-dimethylthiazol-2-yl)-5-(3-carboxymethoxyphenyl)-2-(4-sulfophenyl)-2H-tetrazolium (MTS) assay validated the proliferation reduction by miR-375-mimic in a dose-dependent manner (25, 50, 100 nM; Figure 2B). To mimic the in vivo tumor microenvironment in which basement membranes separate epithelial cells from stromal tissues, we used extracellular matrix (Matrigel) to determine the potential effect of miR-375 on in vitro tumorigenicity. Cells transfected with miR-375-mimic formed significantly reduced number of and smaller colonies (Figure 2C). Furthermore, remarkable reduction of anchorage-independent cell growth was demonstrated in soft agar colony formation assay for cells transfected with miR-375-mimic but not with miR-375 inhibitor or NS control (Figure 2D). The inhibitory effect of miR-375 on transforming phenotype is consistent with miR-375 being an important tumor suppressor miRNA required to suppress proliferation and colony formation of oral cancer cells.

miR-375 inhibits oral cancer cell migration and invasion

In vitro scratch assay was performed to analyze the effect of miR-375 on the migratory behavior of CAL 27 cells. Migration rate of CAL 27 cells was clearly reduced by miR-375-mimic transfection (Figure 3A). During the 48-h monitoring period, both untreated cells and miR-375 inhibitor–transfected cells completely recovered the wound formed in the in vitro scratch assay. Quantitative analyses of the results indicated that the migration of miR-375 inhibitor–transfected cells was faster at the 24- and 36-h time points compared with untreated cells. On the other hand, the scratched area of miR-375-mimic–transfected cells remained unclosed at the 48-h time point, indicating a slower migration of these cells compared with untreated or miR-375 inhibitor–transfected cells (Figure 3B). Migration and invasion assay were performed using 8-μm–pore size Transwell with or without Matrigel coating, respectively. Consistent with the in vitro scratch assay, the Transwell migration assay indicated a decrease migratory activity by increase of miR-375 level in the cells (Figure 3C). Transwell invasion assay showed a remarkable reduction of invasiveness by miR-375-mimic transfection (Figure 3D). Together these findings indicate that miR-375 inhibits migration and invasion of the cancer cells.

CIP2A is a novel miR-375 target

Several known miR-375 targets were examined in our oral cancer cell model system to test their functional relevance in oral cancer. PDK1 (Tsukamoto *et al.*, 2010), YWHAZ (14-3-3ζ; Tsukamoto *et al.*, 2010), JAK2 (Ding *et al.*, 2010), and HuD (Abdelmohsen *et al.*, 2010) were selected as cancer-associated miR-375 targets to investigate their roles in oral cancers. Among the four targets tested, only PDK1 and 14-3-3ζ levels changed upon modulation of miR-375 level (Supplemental Figures S1 and S2). An average of 20% PDK1 mRNA and 54% 14-3-3ζ mRNA decrease was observed in the miR-375-mimic–transfected cells (Supplemental Figure S1A). Similarly, miR-375-mimic transfection reduced the protein level of PDK1 and 14-3-3ζ in miR-375-mimic–transfected cells by 27 and 31%, respectively (Supplemental Figure S1B). The mRNA levels of PDK1 were elevated in oral tumors (Supplemental Figure S1C), especially in advanced-stage tumors (Supplemental Figure S1D). However, no significant correlation was observed between the expressions of PDK1 and miR-375 in the clinical specimens (Supplemental Figure S1E). The expression levels of 14-3-3ζ mRNA showed no significant difference between normal controls and oral tumors (Supplemental Figure S1F) and the subgroups of tumors (Supplemental Figure S1G). The expressions of 14-3-3ζ and miR-375 were not correlated with each other in oral tissues (Supplemental Figure S1H). Expression level of JAK2 was not specifically altered by miR-375-mimic transfection, and HuD was barely detectable in CAL 27 cells (Supplemental

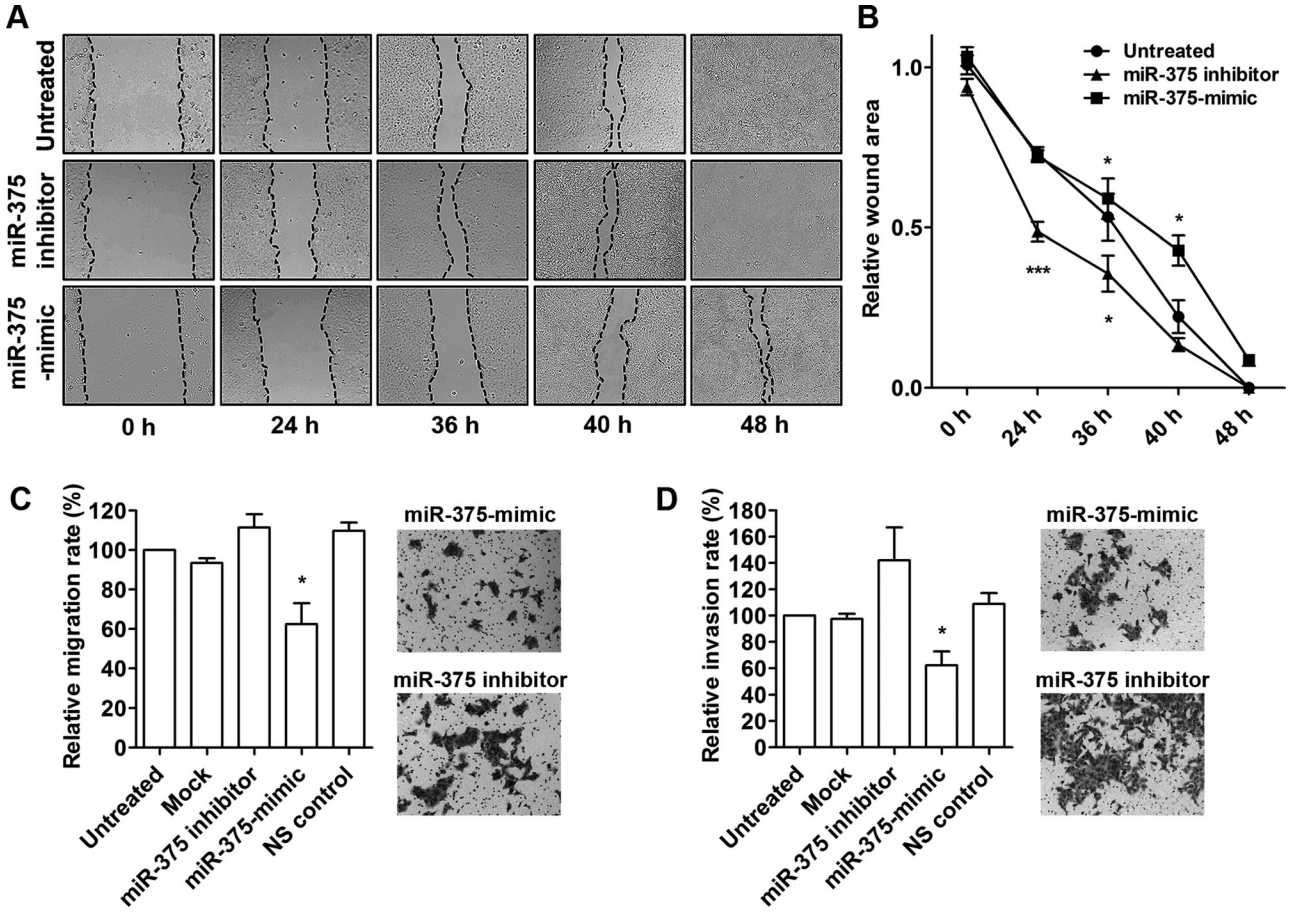

FIGURE 3: miR-375 inhibits oral cancer cell migration and invasion. (A) Representative images of CAL 27 cells were taken at 0, 24, 36, 40, and 48 h during scratch wound-healing assay. Dash lines indicate the initial boundaries of the scratches (0 h) and cell movement leading edges at subsequent time points. (B) Quantitative analysis of the relative wounded area at different time points. The average of the respective wound area was calculated from at least five different random images. (C) Transwell migration assay was performed to examine the effect of miR-375-mimic or inhibitor on CAL 27 cells. After 24 h, the cells on the upper surface were removed and the cells on the lower surface were fixed and stained. Five fields were counted per each filter. (D) Invasion assay was performed using Matrigel-coated Transwell filter. Transfected cells were incubated for 48 h in the filter, and the cells on the upper surface were removed and the cells on the lower surface were fixed and stained the cells on the lower surface were fixed and stained. Five fields were counted per each filter. All results are expressed as mean ± SD from at least three independent experiments. *$p < 0.05$; **$p < 0.01$; ***$p < 0.001$.

Figure S2). These observations led to the identification of a novel miR-375 target relevant to oral cancer.

Our previous studies indicated that CIP2A is overexpressed in oral carcinoma (Katz *et al.*, 2010). Therefore, to postulate the possibility that miR-375 might posttranscriptionally regulate CIP2A transcript, we used bioinformatics to examine whether CIP2A was a potential novel miR-375 target. Several in silico miRNA target prediction programs that predict miRNA binding on 3′ untranslated region (UTR) of targets, including TargetScan (Lewis *et al.*, 2005), PicTar (Krek *et al.*, 2005), starBase (Yang *et al.*, 2011), and miRanda (Enright *et al.*, 2003), did not show CIP2A (KIAA1524) as a miR-375 target. However, it was interesting to note that although the sequences of miR-375 in different mammalian species were highly conserved (Supplemental Figure S3A), the length and sequences of CIP2A 3′ UTR were not similar across these species (Supplemental Figure S3, B and C). These data suggested the possibility that regions other than the 3′ UTR on CIP2A might contain binding sites for miR-375. The RNA22 (Miranda *et al.*, 2006) program, which relies on sequence complementarity between miRNA and targets regardless of the location on the target, was used to explore this possibility. Five highly conserved miR-375 binding sites (A–E) were identified in the coding sequence (CDS) of CIP2A (Figure 4A). The CDS sequence corresponding to miR-375 seed–binding regions (nucleotide positions 2–8) of sites B, C, and E was 100% conserved, site D had a single nucleotide disparity on position 7, and site A had two nucleotide disparities at positions 4 and 7. The close distances between some miR-375–binding sites implied a possible cooperative effect, although site A seemed to contribute less to the repression, whereas other sites had prominent effects on CIP2A regulation (Supplemental Figure S3D). A 1.3-kb CIP2A cDNA clone in our previous study corresponding to position 2119–3425 of KIAA1524 (NM_020890.2; Soo Hoo *et al.*, 2002), which contained all five putative binding sites, was subcloned into a firefly luciferase (FL) reporter construct. The alignment of miR-375 with the sequences of CIP2A is illustrated in Figure 4A.

Using the dual luciferase reporter system, we cotransfected HEK 293 cells with the CIP2A FL construct with or without miR-375-mimic. Compared to the cells transfected with the luciferase

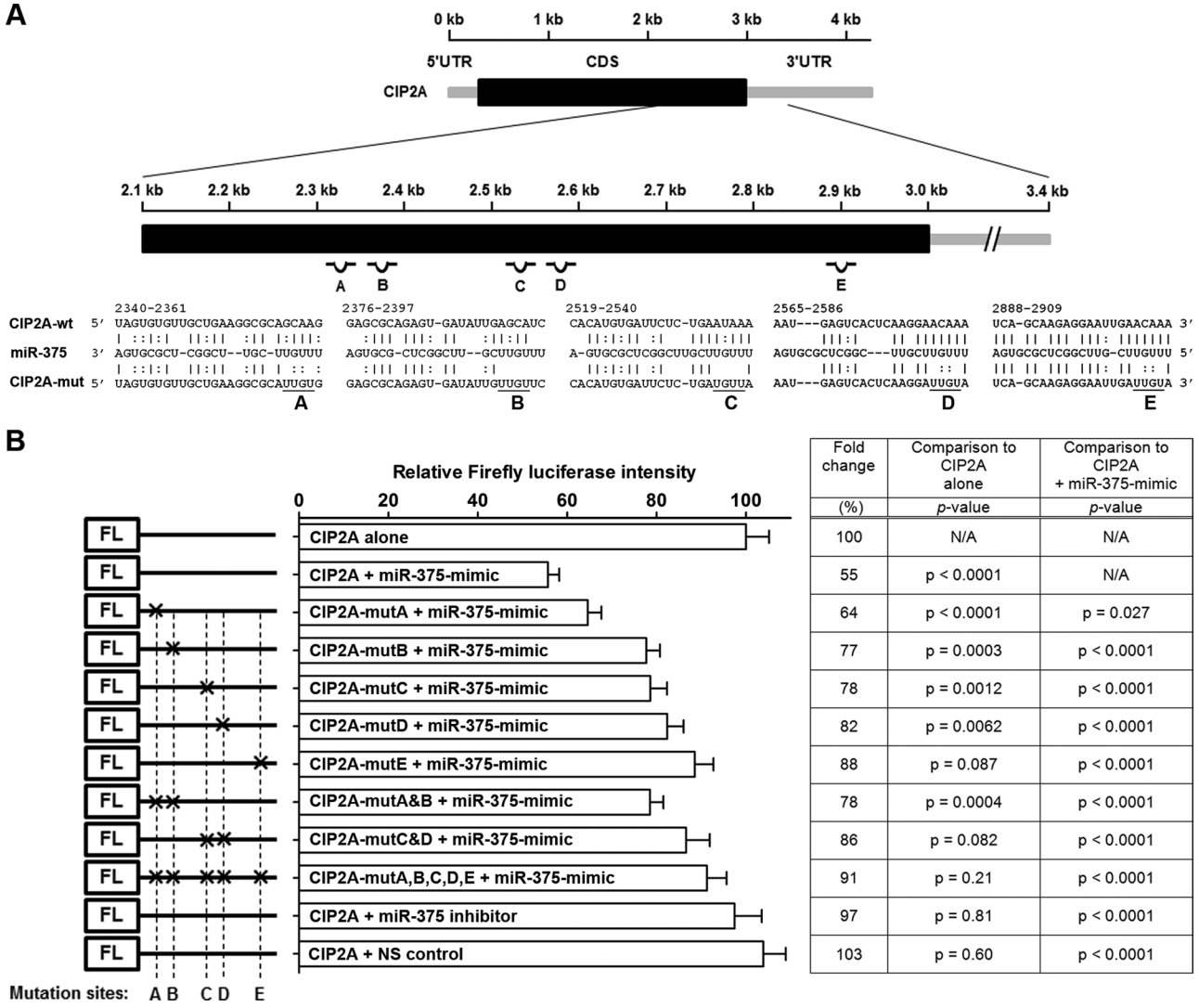

Fold change	Comparison to CIP2A alone	Comparison to CIP2A + miR-375-mimic
(%)	*p*-value	*p*-value
100	N/A	N/A
55	p < 0.0001	N/A
64	p < 0.0001	p = 0.027
77	p = 0.0003	p < 0.0001
78	p = 0.0012	p < 0.0001
82	p = 0.0062	p < 0.0001
88	p = 0.087	p < 0.0001
78	p = 0.0004	p < 0.0001
86	p = 0.082	p < 0.0001
91	p = 0.21	p < 0.0001
97	p = 0.81	p < 0.0001
103	p = 0.60	p < 0.0001

FIGURE 4: CIP2A is directly regulated by miR-375 through multiple binding sites. (A) Five individual miR-375–binding sites were predicted on the CDS of CIP2A. A 1.3-kb CIP2A cDNA containing all putative binding sites was subcloned downstream of FL reporter construct (pMiR-Target). Four nucleotide sequences per seed-binding region for individual sites on CIP2A-CDS were mutated to disrupt the putative miRNA–mRNA interactions. Lines between CIP2A and miR-375 complementary nucleotides are the typical Watson–Crick interactions (A-U and G-C, respectively), and colons are the weak, nontypical base-pair interactions. (B) Luciferase reporter analyses of CIP2A in the presence of miR-375 showing percentages of fold change and the *p* values for each comparison. Dual luciferase assay was used to determine the direct regulation of CIP2A by miR-375. FL constructs were cotransfected with miR-375-mimic or inhibitor or NS control. *Renilla* luciferase was used as an internal control to normalize the expression of FL activity. The mutations are designated as A–E, as indicated. Results were compared with either FL-CIP2A alone or cotransfected with miR-375-mimic for the statistical analyses. All results are expressed as mean ± SD from at least three independent experiments. N/A, not available.

construct alone, cells cotransfected with the miR-375-mimic expressed significantly reduced amount of luciferase activity (100% reduced to 55%), suggesting that miR-375 repressed the expression of CIP2A (Figure 4B, CIP2A alone vs. CIP2A + miR-375-mimic). To identify the relative contribution of each candidate miR-375–binding site, we generated mutations of four nucleotides in each seed-binding site to abrogate the putative miRNA–mRNA interactions (Figure 4A). We examined individual binding-site mutants (CIP2A-mutA to E) for their contribution to the repressive effect by performing cotransfection of individual mutants with miR-375-mimic. Altering these individual binding sites significantly reduced the repression effect by miR-375-mimic. Mutating binding site E exhibited the most prominent interference of the repression effect, similar to the level of transfection without miR-375-mimic (p = 0.087). These results showed that all five putative miR-375–binding sites contribute to the regulation of CIP2A. Previous reports suggested that close distance between miRNA seed–binding sites enhances target down-regulation (Kloosterman *et al.*, 2004; Vella *et al.*, 2004; Saetrom *et al.*, 2007). Therefore the cooperative effects of binding sites in close proximity were examined by generating double mutations of binding sites A and B (32 nucleotides [nt] distant), and C and D (41 nt distant). Despite the reduction of repression effect produced by mutation of C or D alone, each mutation still showed significant repression effect generated

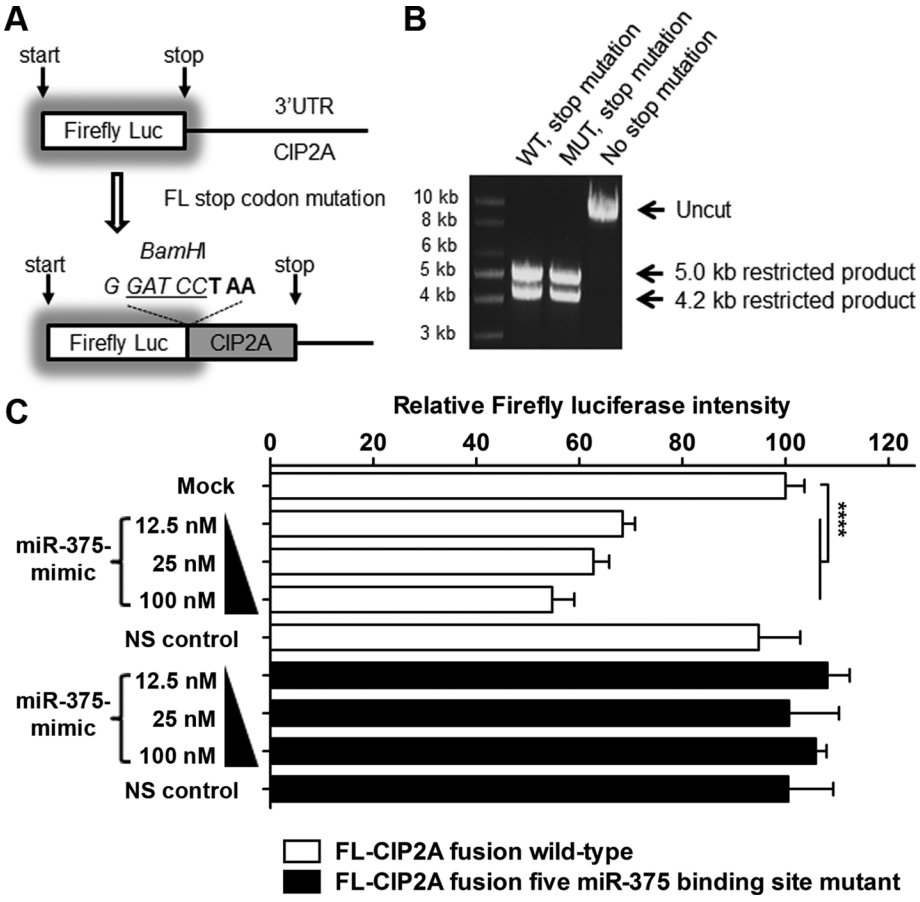

FIGURE 5: miR-375 regulates CIP2A translation by binding to the CDS. (A) Generation of FL-CIP2A in-frame fusion constructs. GATTC sequences inserted upstream of the stop codon of FL shift the frame and generate the fusion construct, creating a new *Bam*HI restriction enzyme site. (B) The *Bam*HI site on the vector backbone and the de novo *Bam*HI site yielded two restricted DNA fragments of 5.0 and 4.2 kb. Electrophoresis was performed on 1% agarose gel. "FL-CIP2A fusion WT" represents the construct with intact miR-375–binding sites, and "FL-CIP2A fusion MUT" represents the construct with mutation of all five miR-375–binding sites. (C) Luciferase reporter analyses of FL-CIP2A in the presence of miR-375-mimic. The WT (white bars) or MUT (black bars) version of FL-CIP2A fusion constructs was cotransfected with miR-375-mimic or NS control. Three different concentrations of miR-375-mimic were used (12.5, 25, 100 nM). *Renilla* luciferase was cotransfected and used as an internal control to normalize the expression of FL activity. Results were compared with either FL-CIP2A transfection alone (mock) or NS control for the statistical analyses. All results are expressed as mean ± SD from at least three independent experiments. ****$p < 0.0001$.

by miR-375-mimic (78 and 82%, respectively). When combinatorial mutation of the C and D sites was generated, the luciferase activity was not significantly repressed in spite of the cotransfection of miR-375-mimic (86%, $p = 0.082$), indicating that the cooperative effect of sites C and D was important for miR-375–mediated regulation for CIP2A (Figure 4B). When cells were transfected with luciferase construct with all five binding sites mutated, miR-375-mimic did not affect the luciferase activity and instead showed similar activity to the cells transfected with CIP2A alone or with miR-375 inhibitor or NS control (Figure 4B). These results demonstrated that miR-375 directly regulated CIP2A through five binding sites located on the CDS.

miR-375 regulates CIP2A translation by binding to the CDS

Despite the obvious repression effect through direct interaction between miR-375 and CIP2A illustrated in Figure 4, the relevance of miR-375 repressing CIP2A by targeting the CDS remained unclear because data shown in Figure 4 could be interpreted as miR-375 repression of binding sites in the 3′ UTR downstream of the reporter FL CDS. To demonstrate that miR-375 regulates these five binding sites, which are located in CDS, a FL-CIP2A in-frame fusion protein was generated by inserting five nucleotides (GATCC) immediately upstream of the stop codon of FL (Figure 5A). The design was such that successful mutants would inactivate the stop codon and generate an extra *Bam*HI restriction site to facilitate the screening process. Restriction digestion of mutant plasmids with *Bam*HI generated two DNA fragments of 5.0 and 4.2 kb derived from cutting the preexisting *Bam*HI restriction site in the plasmid and the newly created *Bam*HI site (Figure 5, A and B). FL-CIP2A fusion constructs were generated for both wild-type (WT, with five intact miR-375–binding sites) and mutant (MUT, five mutated miR-375–binding sites) forms (Figure 5B). Dual luciferase assay showed that luciferase activity decreased by miR-375-mimic and FL-CIP2A-WT cotransfection in a dose-dependent manner (Figure 5C). In contrast, the luciferase activity was not affected in miR-375-mimic and FL-CIP2A MUT cotransfection, indicating that the repression of FL was specific to miR-375–mediated CIP2A regulation (Figure 5C).

miR-375 regulates CIP2A and MYC expression

In the same patient cohort used for measuring miR-375 levels (shown in Figure 1), an increased expression of CIP2A mRNA levels was observed in tumors compared with normal controls (Figure 6A). In particular, advanced-stage tumors expressed a higher level of CIP2A, indicating the critical function of CIP2A in the development of oral cancer (Figure 6B). The normal controls and advanced tumors showed an inverse correlation for the level of CIP2A and miR-375 ($p = 0.03$, Figure 6C). Of interest, significant inverse correlation was observed between CIP2A and miR-375 expression in NCI-60 cells, which are 60 established cell lines derived from nine different cancer tissues of origin (breast, CNS, colon, leukemia, melanoma, non–small cell lung cancer, ovarian, prostate, and renal; $p = 0.01$; Figure 6D). This result was analyzed from genome-wide mRNA and miRNA profiling data using NCI-60 cell lines (Reinhold *et al.*, 2012). Seven head and neck cancer cell lines examined in this study also showed an inversely correlated pattern but not at a statistically significant level, due to the small sample sizes (inset of Figure 6D). Cells transfected with miR-375-mimic exhibited reduced cytoplasmic expression of CIP2A compared with miR-375 inhibitor–transfected cells (Figure 6E). In addition, 31% reduction of CIP2A mRNA (Figure 6F) and 48% decrease of protein levels (Figure 6G) were observed in CAL 27 cells transfected with miR-375-mimic. Because CIP2A is known to prevent MYC degradation, we examined MYC expression and detected 46% reduction in the miR-375-mimic–transfected CAL 27 cells (Figure 6G).

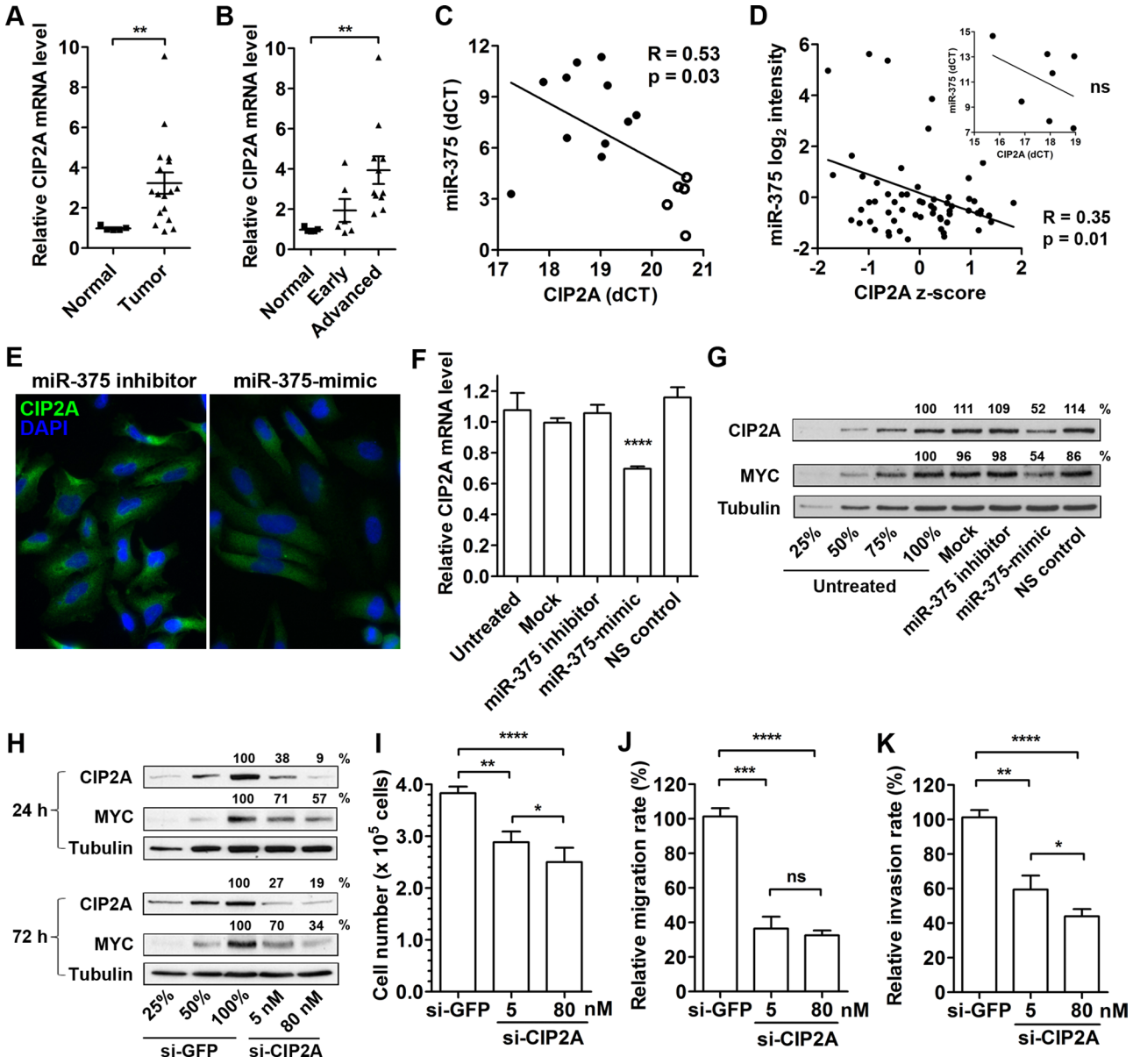

FIGURE 6: miR-375 regulates CIP2A and MYC expression. (A) Oral tumors had significantly higher CIP2A mRNA level than normal tissues. (B) Advanced-stage tumors had significantly higher CIP2A level compared with normal. (C) Significant inverse correlation was observed in linear regression analyses between miR-375 and CIP2A in normal controls and advanced-stage tumors ($R = 0.53$, $p = 0.03$). Closed and open circles indicate 11 advanced tumors and five normal controls, respectively. (D) Significant inverse correlation was observed between CIP2A and miR-375 expression in NCI-60 cell lines ($R = 0.35$, $p = 0.01$). A similar comparison in seven head and neck cancer cell lines did not reveal a significant p value (ns), despite a similar inverse correlation pattern (inset). (E) Reduced cytoplasmic expression of CIP2A in HeLa cells transfected with 25 nM miR-375-mimic compared with cells transfected with 25 nM miR-375 inhibitor for 48 h. CIP2A staining was detected by mouse monoclonal anti-CIP2A, followed by Alexa 488 goat anti-mouse immunoglobulin (green). Representative images for 40× magnification. Nuclei were counterstained with DAPI (blue). (F) The mRNA level of CIP2A in CAL 27 cells transfected with miR-375-mimic for 72 h were significantly reduced compared with other control groups. All results are expressed as mean ± SD from at least three independent experiments. (G) Significant repression of protein levels of CIP2A were observed, 27 and 31%, respectively, in the miR-375-mimic–transfected cells compared with the untreated cells. To calibrate the semiquantitative measurement, 25, 50, 75, and 100% of untreated cell lysates were included in the Western blot. (H) Western blot analysis of CIP2A and MYC protein levels 24 and 72 h after si-CIP2A transfection in CAL 27 cells. si-CIP2A was transfected at 5 and 80 nM, respectively. si-GFP was used as a control, and 25, 50, and 100% of si-GFP transfected cell lysate were loaded for semiquantitative analysis. (I) Live CAL 27 cells 72 h posttransfection with si-GFP or si-CIP2A counted by trypan blue exclusion staining. CAL 27 cells transfected with si-GFP or si-CIP2A for 24 h were trypsinized and analyzed in a Transwell migration assay after 24 h (J) and Matrigel-coated Transwell invasion assay after 48 h (K). All results are expressed as mean ± SD from three independent experiments. ns, not significant; *$p < 0.05$; **$p < 0.01$; ***$p < 0.001$; ****$p < 0.0001$.

To further investigate the functional effects of miR-375–mediated regulation of CIP2A and MYC in oral cancer, we used small interfering RNA (siRNA) knockdown of CIP2A to evaluate the consequences on cancer properties. After transfection of siRNA targeting CIP2A (si-CIP2A) or green fluorescent protein (si-GFP), we performed cell proliferation, migration, and invasion assays (Figure 6, H–K). Two concentrations (5 and 80 nM) of si-CIP2A were used with si-GFP as a negative control, and protein levels were measured at 24 and 72 h posttransfection to ensure that the si-CIP2A effects continued throughout the assay. Compared to the cells transfected with si-GFP, Western blot analysis showed a dramatic decrease of CIP2A and MYC levels (with 80 nM showing a stronger silencing effect than 5 nM) at 24 h posttransfection of si-CIP2A, and this repression continued at 72 h posttransfection (Figure 6H). Knockdown of CIP2A and corresponding decrease in MYC levels affected cancer traits. Transfection of si-CIP2A in both concentrations effectively reduced the cell proliferation rate in 72 h, and use of 80 nM si-CIP2A was significantly more effective in reducing proliferation (Figure 6I). The Transwell assay was used for migration and invasion properties. After 24-h transfection of siRNAs, cells were trypsinized and plated in the Transwell. Migration rate was monitored after 24 h, and ~60% reduction of migration was observed in both 5 and 80 nM si-CIP2A–transfected cells (Figure 6J and Supplemental Figure S4). The invasion rate was examined 72 h posttransfection to provide additional time for the cells to invade through the Matrigel-coat layer. Both si-CIP2A concentrations effectively reduced the invasion rate compared with si-GFP–transfected cells, whereas 80 nM of si-CIP2A exhibited a significantly stronger inhibition effect than 5 nM transfection (Figure 6K and Supplemental Figure S4). Together these data suggest that miR-375 plays a crucial role in regulating CIP2A in oral cancer, as illustrated in Figure 7.

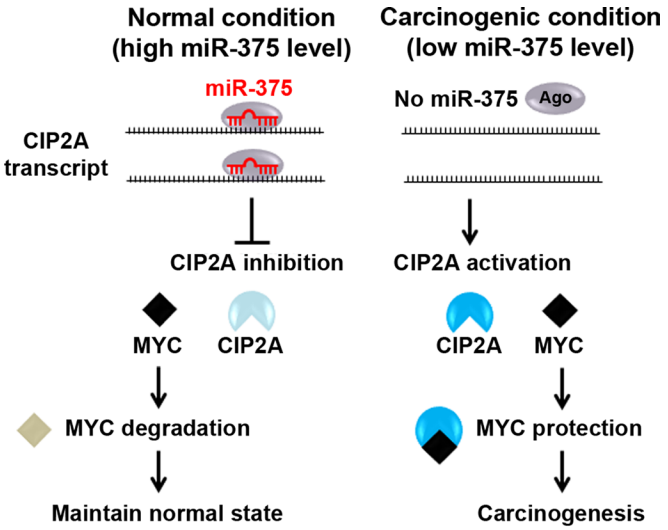

FIGURE 7: Overall schematic model of miR-375 as a tumor suppressor by regulating CIP2A and MYC. In normal physiological condition in which miR-375 levels are high, CIP2A protein translation is negatively regulated by miR-375–mediated posttranscriptional regulation on CIP2A transcripts. As a result, unprotected MYC proteins are subjected to proteolytic degradation and cell proliferation is controlled. In contrast, cells under carcinogenic conditions express low levels of or no miR-375 and fail to efficiently regulate CIP2A expression. MYC proteins are secured by CIP2A proteins from degradation. As a consequence, an increase of MYC stability promotes uncontrolled cell growth and proliferation, resulting into accelerating cancer development.

DISCUSSION

Animal miRNAs are known to have an imperfect interaction with the target 3′ UTR recognized by a perfect match of nucleotides 2–7, the "seed" sequence of miRNAs (Lewis *et al.*, 2005). Although the majority of human miRNA studies focus on the 3′ UTR of target genes, recent theoretical and computational approaches show that miRNAs also interact with the 5′ UTR or CDS (Miranda *et al.*, 2006; Lytle *et al.*, 2007; Zhou *et al.*, 2009; Nelson *et al.*, 2011; Reczko *et al.*, 2012). Consistent with our study, several functional studies experimentally validated these CDS-targeting miRNAs and thus indicate a need for more in-depth studies regarding how commonly these predictions reflect functional interactions with CDS in human diseases (Duursma *et al.*, 2008; Forman *et al.*, 2008; Tay *et al.*, 2008; Pan *et al.*, 2010; Ott *et al.*, 2011). For example, human miR-148a represses DNA methyltransferase 3b gene expression (Duursma *et al.*, 2008), combination of miR-134, miR-296, and miR-470 modulates the expression of stem cell markers Nanog, Oct4, and Sox2 (Tay *et al.*, 2008), and let-7 directly targets miRNA-processing enzyme Dicer (Forman *et al.*, 2008). These miRNA–mRNA binding sites were all located on the CDS of respective targets. It is intriguing that the length of CIP2A 3′ UTR varies among mammalian species, and sequence similarity of 3′ UTR is low except between humans and chimpanzees. This shows that the 3′ UTR of CIP2A is not evolutionarily conserved and suggests the possibility that the CDS, instead of the 3′ UTR, is targeted for miRNA-mediated regulation.

In contrast to animal miRNAs, many plant miRNAs interact with target CDS with "high-sequence complementarity" and elicit RNA interference–mediated direct mRNA cleavage (Llave *et al.*, 2002; Rhoades *et al.*, 2002). It is important to note that although miR-375–binding sites locate on the CDS of CIP2A, the sites interact like typical animal miRNA binding rather than the "high-sequence complementarity" observed in plants. Regarding this feature, the reduction of miR-375–mediated CIP2A expression was more prominent in protein levels (48% reduced) than mRNA levels (31% reduced; Figure 6), suggesting that miR-375 induces both translational repression and mRNA degradation.

Another unique feature of miR-375 binding to CIP2A CDS is the existence of five sites, which is apparently critical because lack of individual sites, as demonstrated by specific mutagenesis, significantly reduced the relative repression of FL activity (Figure 4). It is reasonable to speculate that CIP2A is under tight regulation by miR-375 to ensure its suppression in normal physiological conditions. Regulation by multiple miRNA-binding sites is important because miRNA-binding sites in CDS mediated repression less effectively than in the 3′ UTR (Baek *et al.*, 2008; Selbach *et al.*, 2008). Thus it is reasonable that the multiple miR-375–binding sites have synergistic effects in regulating CIP2A through the CDS, as suggested by previous reports (Saetrom *et al.*, 2007; Fang and Rajewsky, 2011).

Many miRNA studies in cancer research identified deregulated oncomirs or tumor suppressor miRNAs involved in misregulated gene expression in human malignancies. For example, elevated expression of miR-21 in tongue (Jung *et al.*, 2012), breast (Si *et al.*, 2007), or lung (Seike *et al.*, 2009) behaves as an oncomir, which promotes tumorigenesis by targeting tumor suppressor genes. In contrast, expression of tumor suppressor miRNAs, such as miR-34a (Tazawa *et al.*, 2007; Yamakuchi *et al.*, 2008) or let-7 (Johnson *et al.*, 2005; Kumar *et al.*, 2008), is reduced in various types of cancers. Examination of the expression of miRNAs and identification of their

targets is crucial for understanding the gain or loss of function of deregulated miRNAs. Recent studies reported underexpression of miR-375 in head and neck cancer (Avissar *et al.*, 2009; Hui *et al.*, 2011; Nohata *et al.*, 2011; Harris *et al.*, 2012), as well as in other types of cancer, such as cervical cancer (Wang *et al.*, 2011), hepatocellular cancer (Ladeiro *et al.*, 2008), esophageal cancer (Kong *et al.*, 2012), and gastric cancer (Ding *et al.*, 2010; Tsukamoto *et al.*, 2010). This suggests that miR-375 may behave as a tumor suppressor in cancers. Although other miR-375–mediated regulatory functions in oral cancers remain to be understood, the presented study demonstrated how miR-375 functions as a tumor suppressor by regulation of CIP2A. Furthermore, our correlation study on NCI-60 cell lines indicates a need for extended research on whether the miR-375–mediated regulatory mechanism on CIP2A is involved in other cancers.

Taken together, the results in this work demonstrated the importance of miR-375 as a tumor suppressor in oral cancer by regulating CIP2A and suppressing MYC expression. This study is the first to identify miRNA-mediated regulation of CIP2A. The direct correlation between miR-375 and CIP2A through interactions with five highly conserved sites in the CDS of CIP2A suggests a regulatory mechanism that might not be limited to oral cancer but also apply to various types of cancers. The function of CIP2A in maintaining the growth and proliferation of cancer cells is critical, considering that MYC is deregulated in a wide variety of cancers (Dang, 2012). As summarized in Figure 7, in normal conditions, CIP2A is repressed by the high level of miR-375 and MYC proteins are subjected to proteolytic degradation mediated by PP2A due to the low level of CIP2A protein. In contrast, when the tumor suppressor miR-375 is absent in carcinogenic conditions, posttranscriptional regulation of CIP2A is abolished, and this contributes to the protection of MYC from degradation. As a result, increased MYC levels promote uncontrolled cell growth and proliferation, which facilitates carcinogenesis. Therefore miR-375 plays a critical guardian role in oral epithelial cells, and lack of this molecule might lead to carcinogenesis and tumor progression. Our data thus suggest an attractive potential therapeutic target for oral cancer and other miR-375–deficient cancers.

MATERIALS AND METHODS

Patient samples and cell lines

Human oral tissues were collected from the H. Lee Moffitt Cancer Center (Tampa, FL; Protocol MCC-15730) and approved by the Institutional Review Board of the University of South Florida (106444). Cell lines CAL 27, FaDu, SCC-25, and RPMI 2650 were purchased from the American Type Culture Collection (Manassas, VA); HN and BHY were purchased from DSMZ (Braunschweig, Germany); OQ01 was a primary cultured head and neck cancer cell line. Detail information on tissue samples and cell culture conditions is available from our previous study (Jung *et al.*, 2012). In brief, total RNAs isolated from normal tongues and oral tumors were used for miRNA array analysis, and normalized microarray data were submitted to the Gene Expression Omnibus archive (accession number GSE28100; Jung *et al.*, 2012). Clinicopathological characteristics of these 17 patients were used to define early ($n = 6$) vs. advanced stage ($n = 11$; Jung *et al.*, 2012).

Transfection and quantitative real-time PCR

Cells were transfected with 25 nM of miR-375-mimic, miR-375 inhibitor, or NS control. The NS control is the mirVana miRNA-mimic negative control. All reagents were purchased from Life Technologies (Carlsbad, CA). CIP2A siRNA (5′-CUGUGGUUGUGUUUGCACUdTdT-3′) was designed (Junttila *et al.*, 2007) and synthesized from Thermo Fisher Scientific (Waltham, MA). GFP siRNA (D-001300–01–20; Thermo Fisher Scientific) was used as a control. Lipofectamine 2000 was used for transfections according to the protocol of the manufacturer. All RNA used in this study was isolated using mirVana miRNA Isolation kit (Life Technologies) and was reverse transcribed as previously described (Jung *et al.*, 2012). All supplies for TaqMan microRNA/gene assays were purchased from Life Technologies, and real-time PCR was performed according to the protocol of the manufacturer. Fold changes were calculated using the $2^{-\Delta\Delta Ct}$ method (Pfaffl, 2001). U6 small nuclear RNA and 18S rRNA were used as internal controls for miRNAs and mRNAs, respectively.

Proliferation assays

Transfected cells were trypsinized 72 h posttransfection and counted by trypan blue exclusion staining. In addition, cell proliferation rates were measured by MTS assay using the CellTiter 96 AQueous One Solution Cell Proliferation Assay (Promega, Madison, WI) according to the protocol of the manufacturer. Briefly, 1×10^4 cells were transfected in 96-well plate, and the assay was performed 72 h posttransfection. Three different concentrations (25, 50, and 100 nM) of miR-375-mimic or NS control were used for transfection.

Three-dimensional culture assay

Three-dimensional on-top assay was performed as described previously with minor modification (Lee *et al.*, 2007). Briefly, 1:1 diluted Matrigel (BD Biosciences, San Jose, CA) in DMEM was incubated on a plate at 37°C to allow for polymerization of the gel matrix before incubation of the cells. CAL 27 cells transfected with miR-375-mimic or inhibitor or NS control were trypsinized and resuspended in complete growth medium. Cells were seeded on the surface of Matrigel-coated wells, examined daily, and documented by photographic images after 4 d. Colony counts and diameters were determined by five random nonoverlapping images from each slide.

Soft agar colony formation assay

Transfected cells were trypsinized and resuspended in culture medium containing 0.3% agar, and the agar–cell mixture was plated on top of a bottom layer with 0.5% agar-medium mixture. Images of the plates were photographed after 14 d. The colonies were quantified by counting five random nonoverlapping images.

In vitro scratch assay

The in vitro scratch assay was performed to monitor the directional cell migration rate (Liang *et al.*, 2007). CAL 27 cells were seeded on a six-well plate and transfected with miR-375-mimic or miR-375 inhibitor. Transfected cells were incubated until the confluency reached 100% and then were scratched by a sterile 200-µl pipette tip. Cells were washed three times with phosphate-buffered saline (PBS), cultured, and monitored for 48 h. Images of the wounded area were taken at 0, 24, 36, 40, and 48 h. At least five random nonoverlapping images per experiment were analyzed and quantitated using ImageJ software (National Institutes of Health, Bethesda, MD).

Cell migration and invasion assay

Cell migration and invasion assays were carried out using Transwell chambers (8 µm; Corning Costar, Cambridge, MA). A total of 5×10^4 cells transfected with miR-375-mimic or inhibitor or NS control or siRNAs were suspended in 200 µl of serum-free DMEM in the uncoated (migration assay) or 1:10 diluted Matrigel-coated (invasion

assay) upper chamber. Ten percent fetal bovine serum containing DMEM was added in the lower chamber. After 24 h (migration assay) or 48 h (invasion assay), the upper surface of the filters was cleaned with cotton swabs and the lower surface was fixed and stained with 0.05% crystal violet in 20% methanol for 5 min. Five fields were counted per filter.

Western blot analysis

Western blot analyses were performed as previously described (Jung *et al.*, 2012). The membranes were incubated in 1:500 mouse anti-MYC (9E-10; Santa Cruz Biotechnology, Santa Cruz, CA), 1:200 mouse monoclonal anti-CIP2A (2G10; Novus Biologicals, Littleton, CO), 1:5000 mouse anti-tubulin antibodies (T9026; Sigma-Aldrich, St. Louis, MO), 1:3000 rabbit anti-YWHAZ (C-16; Santa Cruz Biotechnology), 1:1000 rabbit anti-PDK1 (3062; Cell Signaling Biotechnology, Danvers, MA), 1:1000 rabbit anti-JAK2 (06–255; Millipore, Billerica, MA), or 1:100 mouse anti-HuD (H-9; Santa Cruz Biotechnology). Secondary antibodies conjugated to horseradish peroxidase were used at 1:10,000 dilutions (Southern Biotech, Birmingham, AL).

Indirect immunofluorescence

Transfection was performed on eight-well chamber slides, fixed with 3% paraformaldehyde in PBS for 10 min, permeabilized with 0.5% Triton-X/PBS for 5 min, and washed three times in PBS. Cells were incubated with mouse anti-CIP2A monoclonal antibody for 1 h. After washing with PBS, the cells were incubated 45 min with Alexa 488 fluorochrome–conjugated secondary antibody and were counterstained with 4′,6-diamidino-2-phenylindole (DAPI).

Bioinformatics tools

Putative binding sites for miR-375 on CIP2A were predicted using RNA22 (Miranda *et al.*, 2006). The Clustal Omega (www.ebi.ac.uk/Tools/msa/clustalo) multiple alignment program was used for sequence comparison. The National Center for Biotechnology Institute HomoloGene database (www.ncbi.nlm.nih.gov/homologene) was used to obtain homologue information for CIP2A in different species. The mature miR-375 sequence information was obtained from miRBase (www.mirbase.org).

Construction of reporter plasmids

A 1.3-kb CIP2A cDNA fragment used in our previous study (Soo Hoo *et al.*, 2002) contained all five predicted miR-375–binding sites. This cDNA fragment was subcloned between *Eco*RI and *Not*I restriction enzyme sites downstream of the firefly luciferase coding sequence of pMiR-Target vector (OriGene Technologies, Rockville, MD). Four consecutive nucleotides on the seed–binding sites were mutated to disrupt the miRNA–mRNA interaction. Mutagenesis was performed using the QuikChange Site-Directed Mutagenesis Kit and QuikChange Multi Site-Directed Mutagenesis Kit (Stratagene, La Jolla, CA). To generate a construct encoding FL-CIP2A in-frame fusion protein, five nucleotides (GATCC) were inserted immediately upstream of the stop codon (TAA) of FL via insertional mutagenesis. All mutated sequences were confirmed by DNA sequencing. All the primers used for cloning luciferase constructs are listed in Supplemental Table S1.

Dual luciferase assay

HEK 293 cells transfected with luciferase reporters and miR-375-mimic or inhibitor or NS control were harvested after 48 h. The luciferase activities were measured using the Dual-Luciferase Reporter Assay System (Promega) and FLUOstar OPTIMA (BMG Labtech, Germany). *Renilla* luciferase expression levels were used as an internal control to normalize the relative expressions of FL (Jung *et al.*, 2012).

Statistical analyses

Values of the quantitative real-time PCR data using tissue samples were analyzed by the Mann–Whitney *U* test. A two-tailed Student's *t* test was used for all in vitro experiments and expressed as mean ± SD from at least three independent experiments. The statistical analyses were performed using Prism 4.0 (Graph Pad Software, La Jolla, CA).

ACKNOWLEDGMENTS

We thank members of the Chan laboratory for technical assistance, discussion, and encouragement. We are grateful to tissue procurement at H. Lee Moffitt Cancer Center for providing specimens. We also thank Jukka Westermarck for constructive discussions. This work was supported in part by an Alumni Graduate Fellowship (H.M.J.), the Andrew J. Semesco Foundation (H.M.J., E.K.L.C.), and a University of Florida/Moffitt Collaborative Initiative grant (E.K.L.C).

REFERENCES

Abdelmohsen K *et al.* (2010). miR-375 inhibits differentiation of neurites by lowering HuD levels. Mol Cell Biol 30, 4197–4210.

Ambros V (2004). The functions of animal microRNAs. Nature 431, 350–355.

Avissar M, Christensen BC, Kelsey KT, Marsit CJ (2009). MicroRNA expression ratio is predictive of head and neck squamous cell carcinoma. Clin Cancer Res 15, 2850–2855.

Baek D, Villen J, Shin C, Camargo FD, Gygi SP, Bartel DP (2008). The impact of microRNAs on protein output. Nature 455, 64–71.

Bartel DP (2009). MicroRNAs: target recognition and regulatory functions. Cell 136, 215–233.

Come C *et al.* (2009). CIP2A is associated with human breast cancer aggressivity. Clin Cancer Res 15, 5092–5100.

Dang CV (2012). MYC on the path to cancer. Cell 149, 22–35.

Ding L *et al.* (2010). MiR-375 frequently downregulated in gastric cancer inhibits cell proliferation by targeting JAK2. Cell Res 20, 784–793.

Dong QZ, Wang Y, Dong XJ, Li ZX, Tang ZP, Cui QZ, Wang EH (2011). CIP2A is overexpressed in non–small cell lung cancer and correlates with poor prognosis. Ann Surg Oncol 18, 857–865.

Duursma AM, Kedde M, Schrier M, le Sage C, Agami R (2008). miR-148 targets human DNMT3b protein coding region. RNA 14, 872–877.

Enright AJ, John B, Gaul U, Tuschl T, Sander C, Marks DS (2003). MicroRNA targets in *Drosophila*. Genome Biol 5, R1.

Esquela-Kerscher A, Slack FJ (2006). Oncomirs—microRNAs with a role in cancer. Nat Rev Cancer 6, 259–269.

Fang Z, Rajewsky N (2011). The impact of miRNA target sites in coding sequences and in 3′UTRs. PLoS One 6, e18067.

Fernandez PC, Frank SR, Wang L, Schroeder M, Liu S, Greene J, Cocito A, Amati B (2003). Genomic targets of the human c-Myc protein. Genes Dev 17, 1115–1129.

Forman JJ, Legesse-Miller A, Coller HA (2008). A search for conserved sequences in coding regions reveals that the let-7 microRNA targets Dicer within its coding sequence. Proc Natl Acad Sci USA 105, 14879–14884.

Friedman RC, Farh KK, Burge CB, Bartel DP (2009). Most mammalian mRNAs are conserved targets of microRNAs. Genome Res 19, 92–105.

Funk GF, Karnell LH, Robinson RA, Zhen WK, Trask DK, Hoffman HT (2002). Presentation, treatment, and outcome of oral cavity cancer: a National Cancer Data Base report. Head Neck 24, 165–180.

Garzon R, Marcucci G, Croce CM (2010). Targeting microRNAs in cancer: rationale, strategies and challenges. Nat Rev Drug Discov 9, 775–789.

Harris T *et al.* (2012). Low-level expression of miR-375 correlates with poor outcome and metastasis while altering the invasive properties of head and neck squamous cell carcinomas. Am J Pathol 180, 917–928.

Howlader N *et al.* (2012). SEER Cancer Statistics Review, 1975–2009. Available at: http://seer.cancer.gov/csr/1975_2009_pops09/index.html (accessed 2012)

Hui AB *et al.* (2011). Significance of dysregulated metadherin and microRNA-375 in head and neck cancer. Clin Cancer Res 17, 7539–7550.

Jemal A, Bray F, Center MM, Ferlay J, Ward E, Forman D (2011). Global cancer statistics. CA Cancer J Clin 61, 69–90.

Johnson SM *et al.* (2005). RAS is regulated by the let-7 microRNA family. Cell 120, 635–647.
Jung HM, Phillips BL, Patel RS, Cohen DM, Jakymiw A, Kong WW, Cheng JQ, Chan EK (2012). Keratinization-associated miR-7 and miR-21 regulate tumor suppressor reversion-inducing-cysteine-rich protein with kazal motifs (RECK) in oral cancer. J Biol Chem 287, 29261–29272.
Junttila MR *et al.* (2007). CIP2A inhibits PP2A in human malignancies. Cell 130, 51–62.
Junttila MR, Westermarck J (2008). Mechanisms of MYC stabilization in human malignancies. Cell Cycle 7, 592–596.
Katz J, Jakymiw A, Ducksworth MK, Stewart CM, Bhattacharyya I, Cha S, Chan EK (2010). CIP2A expression and localization in oral carcinoma and dysplasia. Cancer Biol Ther 10, 694–699.
Kloosterman WP, Wienholds E, Ketting RF, Plasterk RH (2004). Substrate requirements for let-7 function in the developing zebrafish embryo. Nucleic Acids Res 32, 6284–6291.
Kong KL, Kwong DL, Chan TH, Law SY, Chen L, Li Y, Qin YR, Guan XY (2012). MicroRNA-375 inhibits tumour growth and metastasis in oesophageal squamous cell carcinoma through repressing insulin-like growth factor 1 receptor. Gut 61, 33–42.
Krek A *et al.* (2005). Combinatorial microRNA target predictions. Nat Genet 37, 495–500.
Kumar MS, Erkeland SJ, Pester RE, Chen CY, Ebert MS, Sharp PA, Jacks T (2008). Suppression of non-small cell lung tumor development by the let-7 microRNA family. Proc Natl Acad Sci USA 105, 3903–3908.
Ladeiro Y, Couchy G, Balabaud C, Bioulac-Sage P, Pelletier L, Rebouissou S, Zucman-Rossi J (2008). MicroRNA profiling in hepatocellular tumors is associated with clinical features and oncogene/tumor suppressor gene mutations. Hepatology 47, 1955–1963.
Lee GY, Kenny PA, Lee EH, Bissell MJ (2007). Three-dimensional culture models of normal and malignant breast epithelial cells. Nat Methods 4, 359–365.
Lewis BP, Burge CB, Bartel DP (2005). Conserved seed pairing, often flanked by adenosines, indicates that thousands of human genes are microRNA targets. Cell 120, 15–20.
Li W, Ge Z, Liu C, Liu Z, Bjorkholm M, Jia J, Xu D (2008). CIP2A is overexpressed in gastric cancer and its depletion leads to impaired clonogenicity, senescence, or differentiation of tumor cells. Clin Cancer Res 14, 3722–3728.
Liang CC, Park AY, Guan JL (2007). In vitro scratch assay: a convenient and inexpensive method for analysis of cell migration in vitro. Nat Protoc 2, 329–333.
Lippman SM, Sudbo J, Hong WK (2005). Oral cancer prevention and the evolution of molecular-targeted drug development. J Clin Oncol 23, 346–356.
Llave C, Xie Z, Kasschau KD, Carrington JC (2002). Cleavage of Scarecrow-like mRNA targets directed by a class of *Arabidopsis* miRNA. Science 297, 2053–2056.
Lu J *et al.* (2005). MicroRNA expression profiles classify human cancers. Nature 435, 834–838.
Lytle JR, Yario TA, Steitz JA (2007). Target mRNAs are repressed as efficiently by microRNA-binding sites in the 5′ UTR as in the 3′ UTR. Proc Natl Acad Sci USA 104, 9667–9672.
Messadi DV, Wilder-Smith P, Wolinsky L (2009). Improving oral cancer survival: the role of dental providers. J Calif Dent Assoc 37, 789–798.
Miranda KC, Huynh T, Tay Y, Ang YS, Tam WL, Thomson AM, Lim B, Rigoutsos I (2006). A pattern-based method for the identification of MicroRNA binding sites and their corresponding heteroduplexes. Cell 126, 1203–1217.
Nelson PT, Wang WX, Mao G, Wilfred BR, Xie K, Jennings MH, Gao Z, Wang X (2011). Specific sequence determinants of miR-15/107 microRNA gene group targets. Nucleic Acids Res 39, 8163–8172.
Nohata N *et al.* (2011). Tumor suppressive microRNA-375 regulates oncogene AEG-1/MTDH in head and neck squamous cell carcinoma (HNSCC). J Hum Genet 56, 595–601.
Ott CE *et al.* (2011). MicroRNAs differentially expressed in postnatal aortic development downregulate elastin via 3′ UTR and coding-sequence binding sites. PLoS One 6, e16250.
Pan W *et al.* (2010). MicroRNA-21 and microRNA-148a contribute to DNA hypomethylation in lupus CD4+ T cells by directly and indirectly targeting DNA methyltransferase 1. J Immunol 184, 6773–6781.
Pfaffl MW (2001). A new mathematical model for relative quantification in real-time RT-PCR. Nucleic Acids Res 29, e45.
Prochownik EV (2008). c-Myc: linking transformation and genomic instability. Curr Mol Med 8, 446–458.
Reczko M, Maragkakis M, Alexiou P, Grosse I, Hatzigeorgiou AG (2012). Functional microRNA targets in protein coding sequences. Bioinformatics 28, 771–776.
Reinhold WC, Sunshine M, Liu H, Varma S, Kohn KW, Morris J, Doroshow J, Pommier Y (2012). CellMiner: a web-based suite of genomic and pharmacologic tools to explore transcript and drug patterns in the NCI-60 cell line set. Cancer Res 72, 3499–3511.
Ren J *et al.* (2011). Expression of CIP2A in renal cell carcinomas correlates with tumour invasion, metastasis and patients' survival. Br J Cancer 105, 1905–1911.
Rhoades MW, Reinhart BJ, Lim LP, Burge CB, Bartel B, Bartel DP (2002). Prediction of plant microRNA targets. Cell 110, 513–520.
Saetrom P, Heale BS, Snove O Jr, Aagaard L, Alluin J, Rossi JJ (2007). Distance constraints between microRNA target sites dictate efficacy and cooperativity. Nucleic Acids Res 35, 2333–2342.
Seike M *et al.* (2009). MiR-21 is an EGFR-regulated anti-apoptotic factor in lung cancer in never-smokers. Proc Natl Acad Sci USA 106, 12085–12090.
Selbach M, Schwanhausser B, Thierfelder N, Fang Z, Khanin R, Rajewsky N (2008). Widespread changes in protein synthesis induced by microRNAs. Nature 455, 58–63.
Shi FD *et al.* (2005). Preferential humoral immune response in prostate cancer to cellular proteins p90 and p62 in a panel of tumor-associated antigens. Prostate 63, 252–258.
Shiboski CH, Shiboski SC, Silverman S Jr (2000). Trends in oral cancer rates in the United States, 1973–1996. Community Dent Oral Epidemiol 28, 249–256.
Si ML, Zhu S, Wu H, Lu Z, Wu F, Mo YY (2007). miR-21-mediated tumor growth. Oncogene 26, 2799–2803.
Soo Hoo L, Zhang JY, Chan EK (2002). Cloning and characterization of a novel 90 kDa 'companion' auto-antigen of p62 overexpressed in cancer. Oncogene 21, 5006–5015.
Sun W, Julie Li YS, Huang HD, Shyy JY, Chien S (2010). microRNA: a master regulator of cellular processes for bioengineering systems. Annu Rev Biomed Eng 12, 1–27.
Tay Y, Zhang J, Thomson AM, Lim B, Rigoutsos I (2008). MicroRNAs to Nanog, Oct4 and Sox2 coding regions modulate embryonic stem cell differentiation. Nature 455, 1124–1128.
Tazawa H, Tsuchiya N, Izumiya M, Nakagama H (2007). Tumor-suppressive miR-34a induces senescence-like growth arrest through modulation of the E2F pathway in human colon cancer cells. Proc Natl Acad Sci USA 104, 15472–15477.
Tsukamoto Y *et al.* (2010). MicroRNA-375 is downregulated in gastric carcinomas and regulates cell survival by targeting PDK1 and 14-3-3zeta. Cancer Res 70, 2339–2349.
van der Waal I, de Bree R, Brakenhoff R, Coebergh JW (2011). Early diagnosis in primary oral cancer: is it possible? Med Oral Patol Oral Cir Bucal 16, e300–e305.
Vella MC, Choi EY, Lin SY, Reinert K, Slack FJ (2004). The *C. elegans* microRNA let-7 binds to imperfect let-7 complementary sites from the lin-41 3′UTR. Genes Dev 18, 132–137.
Volinia S *et al.* (2006). A microRNA expression signature of human solid tumors defines cancer gene targets. Proc Natl Acad Sci USA 103, 2257–2261.
Voorhoeve PM, Agami R (2007). Classifying microRNAs in cancer: the good, the bad and the ugly. Biochim Biophys Acta 1775, 274–282.
Wang F *et al.* (2011). miR-375 is down-regulated in squamous cervical cancer and inhibits cell migration and invasion via targeting transcription factor SP1. Am J Pathol 179, 2580–2588.
Yamakuchi M, Ferlito M, Lowenstein CJ (2008). miR-34a repression of SIRT1 regulates apoptosis. Proc Natl Acad Sci USA 105, 13421–13426.
Yang JH, Li JH, Shao P, Zhou H, Chen YQ, Qu LH (2011). starBase: a database for exploring microRNA-mRNA interaction maps from Argonaute CLIP-Seq and Degradome-Seq data. Nucleic Acids Res 39, D202–D209.
Zhou X, Duan X, Qian J, Li F (2009). Abundant conserved microRNA target sites in the 5′-untranslated region and coding sequence. Genetica 137, 159–164.